acta medica

ORIGINAL ARTICLE

Morphometry in Classification of Hippocampal Sclerosis

Güneş Güner[1]
ORCID: 0000-0002-7338-1524

Figen Söylemezoğlu[1]
ORCID: 0000-0002-8002-5165

[1]Hacettepe University, Faculty of Medicine, Department of Pathology, Ankara, Turkey.

Corresponding Author: Figen Söylemezoğlu
Hacettepe University, Faculty of Medicine, Department of Pathology, Ankara, Turkey.
E-mail: figensoylemezoglu@gmail.com

Received: 1 October 2021, Accepted: 6 September 2022, Published online: 23 September 2022

ABSTRACT

Hippocampal sclerosis (HS) is evaluated in 3 categories by the latest (2013) ILAE classification. The distinction between these categories rely on the histopathological assessment of pyramidal neuron loss in 4 CA sectors. In order to evaluate neuron loss assessment done manually by a neuropathologist, cell counts were carried out from representative photomicrographs of each section. NeuN immunohistochemistry was applied on hippocampus sections of 28 samples of epilepsy surgery, photographed at x100 magnification to represent each of the 4 sectors, and neuron density was calculated per photo. This density data was compared to the pathology reports' diagnoses. HS type 1 cases were predominant (n=23) with few type 2 and type 3 cases (3 and 2, respectively). Percentage of neuron loss calculated per photos, ILAE classification guidelines and pathological diagnoses rendered without any calculation were relatively well-correlated; with HS type 2 and 3 displaying slight changes from recommendations. Data also display accurate pathological diagnoses of HS without special equipment or cell density calculation. HS types 2 and 3 in Turkey may display variant cell density properties which may warrant further clarification.

Keywords: Epilepsy, hippocampus, hippocampal sclerosis, gliosis, NeuN, immunohistochemistry, classification

INTRODUCTION

Epilepsy is a prevalent disease characterized by periodic and unanticipated seizure episodes, many precipitating and etiological factors, and variable seizure frequencies and types. Although much progress has been made in epilepsy diagnosis and therapy, there remains about a third of epilepsy patients that do not respond to current therapy modalities; in these cases epilepsy surgery may be preferred. A relatively recent surgical procedure in our country, epilepsy surgery is a new area for our pathologists, requiring experience in neuropathology and knowledge of neuroanatomy [1,2].

Hippocampal sclerosis (HS) is the prototype of surgically treatable epileptic syndromes; surgery consists of selective amygdalahippocampectomy or amygdalahippocampectomy accompanied by temporal lobectomy [3]. HS is characterized by pyramidal neuron loss and gliosis of variable intensity and location, along with dentate gyrus findings [4,5]. These different histological patterns have been classified in several attempts, the most recent and well-accepted one is the classification offered in 2013 by the International League Against Epilepsy (ILAE) [4]. ILAE 2013 classification renders three categories according to histological patterns and location of pyramidal neuron loss and gliosis (HS type 1 with losses in CA1 and CA4, the CA1-predominant HS type 2 and the CA4 predominant HS type 3) [4].

Although the 2013 ILAE classification is admittedly a semiquantitative scheme depending on patterns and intensity of pyramidal neuron loss, its use is still recommended, as different HS patterns are

considered to be associated with variable etiologies, clinical findings and therapy response, possibly reflecting different epileptogenetic mechanisms [4-7].

In the present study, digitalized microscopic images are annotated and their neuron counts quantified with the aid of computerized image analysis software, in an attempt to assess the feasibility of such computer-aided morphometric techniques in HS subtyping.

METHODS

The study was approved by the Hacettepe University Non-interventional Clinical Research Ethics Board (31/05/2021, 2022/09-67). Twenty-eight cases that underwent epilepsy surgery (amygdalectomy, hippocampectomy, temporal lobectomy) in Hacettepe University Hospitals between 2017-2019 whose samples were assessed and reported by a single neuropathologist (FS) and whose paraffin blocks were readily available were included in the study. Twenty three of these were reported as HS type 1, three were HS type 2 and two were HS type 3 according to 2013 ILAE criteria. NeuN immunohistochemistry was implemented to show intact neurons with a Leica Bond Max autostainer. Briefly, 4-micrometer thick formalin fixed paraffin embedded tissue sections were deparaffinized, rehydrated and endogenous peroxidase blockage was carried out, followed by antigen retrieval at 100 °C with ER2 (EDTA) solution. Primary antibody (NeuN, Zymed, A60, 1/50) was applied for 25 minutes at room temperature. After incubation with the appropriate secondary antibody at room temperature for 90 min, the signals were visualized with DAB chromogen, slides were dehydrated, and hematoxylin counterstaining was applied.

Neu-N immunostained slides were reviewed by a pathologist (GG) on an Olympus BX53 microscope connected to an Olympus CellSens Entry 2.3 image capture – camera system. At x100 magnification, one area representing each CA sector of each HS case was picked and photographed (Fig. 1A). Photomicrographs were visualized with ImageJ [8] and its "Cell Counter" mode was used to manually count NeuN positive cells.

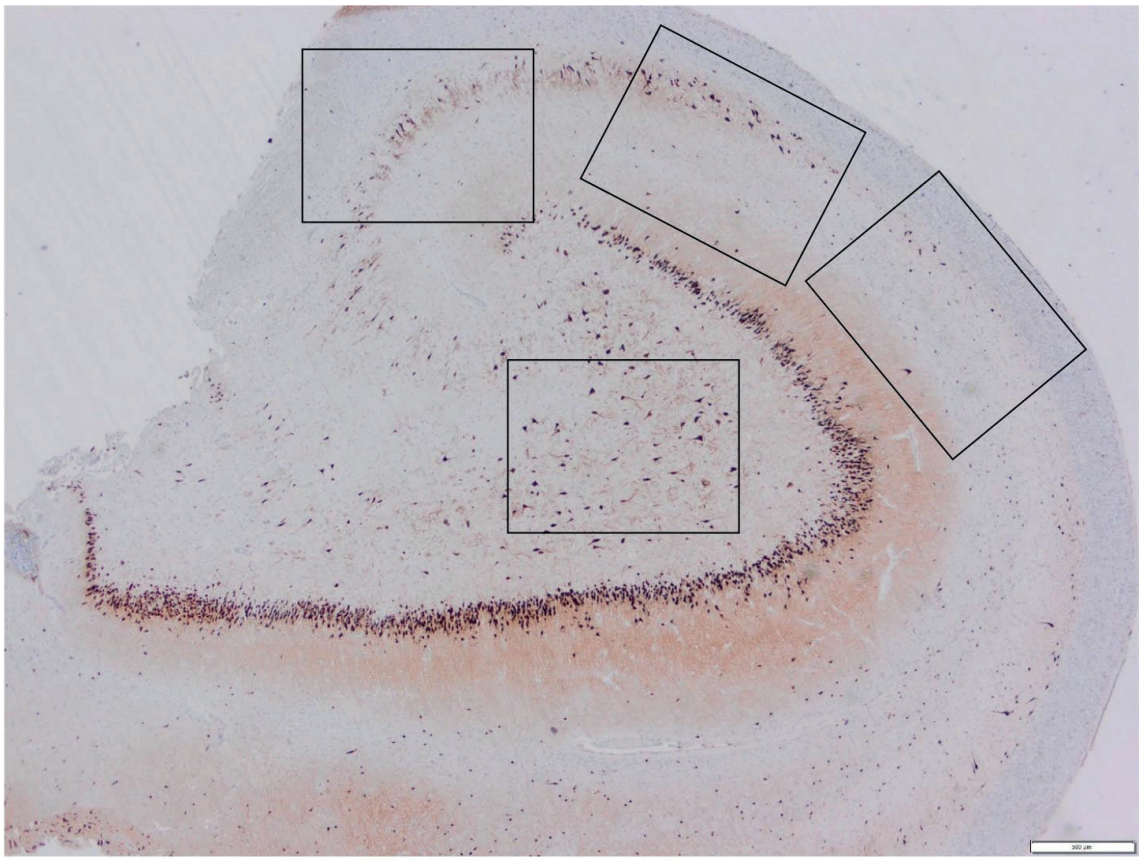

Figure 1A. Representative areas photographed from a Neu-N immunostained hippocampal section (x2.5, HS type 1). ROI for CA4 is shown mid-picture, CA3, CA2 and CA1 are in the upper part of the picture from left ro right, respectively. Scale bar: 500 um.

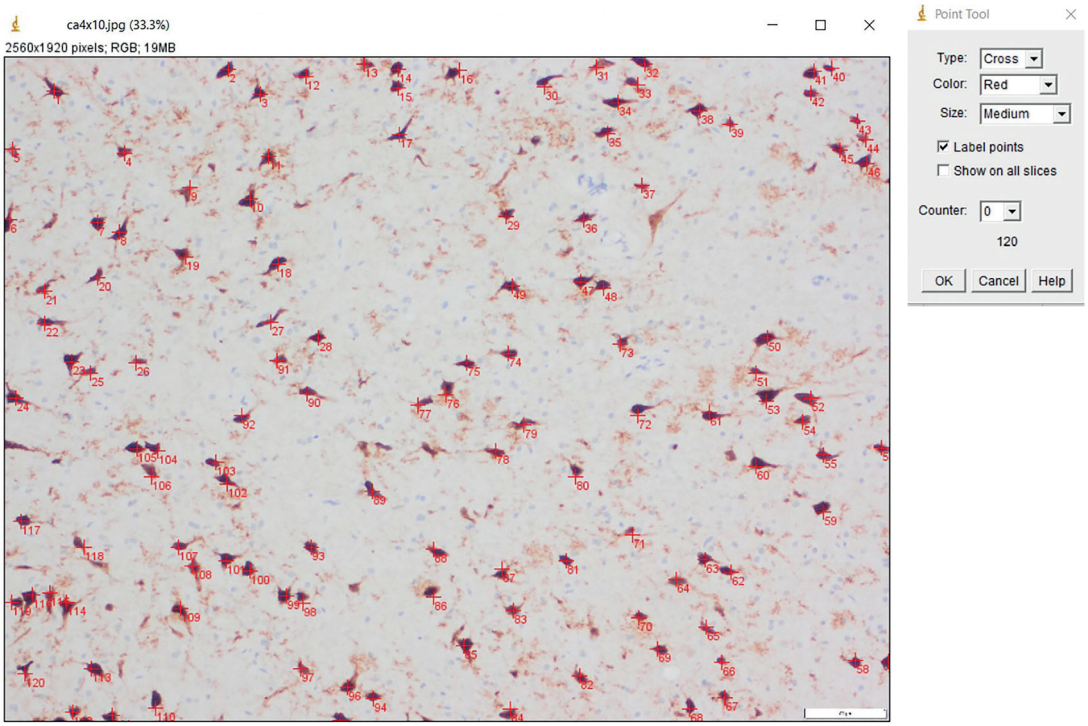

Figure 1B. Manual cell counting of a x10 image with ImageJ. Neu-N immunostaining, x10 magnification. Scale bar: 100 um.

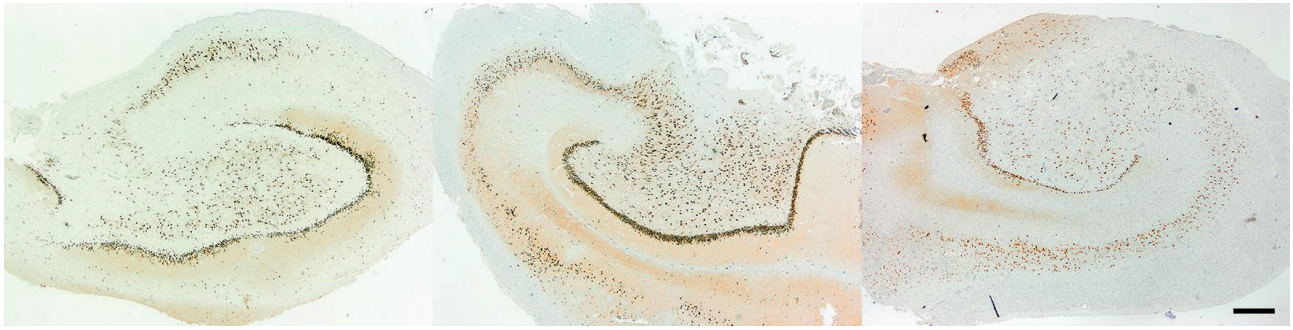

Figure 2. Examples of HS type 1 (left), HS type 2 (mid) and HS type 3 (right). Neu-N immunostaining, x2,5. Scale bar: 500 um.

The number of neurons were divided by the area of the photomicrograph to obtain cell densities (n/mm2) (Fig. 1B). The autopsy cases (n=5) intended to be controls did not react with NeuN antibodies in the immunohistochemistry assay, probably due to prolonged fixation, which prompted the count of neurons on photomicrographs of H-E stained slides. Cell densities were compared via Kruskal-Wallis tests in the R package (Jamovi) [9]. A p value lower than 0,05 was considered statistically significant.

RESULTS

Main clinicopathological features of the cases are shown in Table 1. A low-power (x2,5) view of exemplary HS type 1, HS type 2 and HS type 3 cases are depicted in Fig. 2.

A comparison of neuron loss rates in our cases and the corresponding ILAE criteria [4] is given in Table 2. Sector-based paired comparisons of neuron densities per category are given in Table 3.

Table 1. Major clinicopathological features of the cases with average number of neurons per sector

				Hippocampal neuron counts, mean (min-max)			
Reported diagnosis	n	Sex (M/F)	Average age (min-max)	CA1	CA2	CA3	CA4
HS1	23	13 / 10	20.33 (2-44)	36.2 (1-100)	54.4 (18-121)	37.3 (3-99)	45.9 (4-135)
HS2	3	2 / 1	17.77 (15-22)	72.9 (59-82)	107.04 (99-119)	113.8 (93-132)	204.59 (172-238)
HS3	2	0 / 2	10.5 (10-11)	140.9 (135-147)	96.0 (79-119)	107.7 (69-168)	111.4 (71-175)
Control	5	3 / 2	6.12 (0.17-33)	186.2 (118-253)	135.0 (89-206)	126.0 (75-174)	185.1 (138-268)

Table 2. Average rates of cell loss per sector in cases and the rates of neuron loss in ILAE criteria

DIAGNOSIS	PYRAMIDAL NEURON LOSS (%)			
	CA1	CA2	CA3	CA4
HS1	76.1	56.7	65.8	68.7
ILAE HS1 CRITERIA*	>%80	%30–50	%30–90	%40–90
HS2	61.5	24.3	12.9	-7.9
ILAE HS2 CRITERIA*	APPROX. %80	<%20	<%20	<%25
HS3	26.3	30.2	10.3	35.7
ILAE HS3 CRITERIA*	<%20	<%25	<%30	Approx. %50

* ILAE 2013 [4]

Table 3. P values obtained by sector-by-sector comparisons of HS groups (Dwass-Steel-Critchlow-Fligner)

CA1	HS1	HS2	HS3	Control
HS1	.	0.1	0.097	0.003
HS2	0.1	.	0.307	0.114
HS3	0.097	0.307	.	0.651
Control	0.003	0.114	0.651	.

CA3	HS1	HS2	HS3	Control
HS1	.	0.036	0.226	0.006
HS2	0.036	.	1	0.879
HS3	0.226	1	.	0.98
Control	0.006	0.879	0.98	.

CA2	HS1	HS2	HS3	Control
HS1	.	0.156	0.397	0.012
HS2	0.156	.	0.991	0.724
HS3	0.397	0.991	.	0.651
Control	0.012	0.724	0.651	.

CA4	HS1	HS2	HS3	Control
HS1	.	0.029	0.321	0.003
HS2	0.029	.	0.656	0.879
HS3	0.321	0.656	.	0.866
Control	0.003	0.879	0.866	.

The 23 cases in our HS type 1 category had a rate of 76.1% neuron loss in CA1, 56.7% in CA2, 65.8% in CA3 and 68.7% in CA4. In the HS type 1 category, CA1 and CA4 sectors have considerably less neuron density when compared to controls (p=0.003 in both). Among the three cases of HS type 2 at hand, neuron loss rates were 61.5%, 24.3%, 12.9% in sectors CA1, CA2 and CA3, respectively, while there was no significant neuron loss in CA4. In HS type 2, which is characterized by CA1 neuron loss, there is no statistically significant loss in CA1 sector among our cases (p=0.114). In our HS type 3 group (n=2), CA4 neuron density was not statistically different from the controls (p=0.866). However, the CA4 neuron loss rate of 35.7%, clearly higher than that of other sectors in the HS type 3 category (26.3%, 30.2% and 10.3% losses in sectors CA1, CA2 and CA3 respectively), was noted (Table 2).

DISCUSSION

Histopathology, like in all other acts of pathological assessment, is of paramount importance in HS diagnosis. However, semi-quantitative evaluation, like ILAE criteria, possess the inherent possibility of inter- and intra-observer variability/discrepancy. Most of the time, such variability can be corrected and repeatability enhanced by stepping out of tradition and implementing morphometry-based techniques. Morphometry, in its broadest sense, is the quantitative assessment of size and shape. In pathology, morphometry aims to reach reproducible and accurate data from cell and tissue samples [10]. Technological advances allow for computer-based morphometric analysis of raw data from digitalized slides [11].

With the forthcoming inevitable addition of other modalities such as deep learning and artificial intelligence to this mix, histopathologic subtyping, classification and grading will become experience-independent endeavours [12].

Hippocampus is a part of the archicortex and histologically consists of CA sectors, dentate gyrus, fimbria, subiculum, parasubiculum and entorhinal cortex. In its simplest sense, it is made up of neuronal layers folded into a "C" shape. One of these neuronal layers is the dentate gyrus. The other contains pyramidal neurons and is named the cornu ammonis, due to its resemblance to the horn of the ancient Egyptian god Ammon Ra. Cornu ammonis consists of 4 sectors, numbered consecutively from 1 to 4 [13].

The widely-used ILAE 2013 classification scheme divides HS into three categories depending on pyramidal neuron loss, dentate gyrus neuron loss and gliosis patterns in the 4 CA sectors [4,5]. Despite good interobserver agreement overall, subjectivity is still an issue in semi-quantitative assessment of neuronal loss in different hippocampal sectors [4]. Diagnostic criteria themselves don't reveal stiff cut-off points; for example, for the CA4-dominant HS type 3, criteria suggest neuronal loss rates of <20%, <25%, <30% and "approximately" 50% for sectors CA1, CA2, CA3 and CA4, respectively [4]. For determining the rates of pyramidal neuron loss required by the classification, the reviewer needs to have a visual grasp on the normal neuronal densities of all CA sectors.

The neuron loss rates of the cases reported in our facility are, for the most part, quite close to those recommended by the ILAE 2013 classification [4] (Table 2). In HS type 2 category, our cases displayed a lower percentage of neuron loss than recommended in CA1 sector (61.5% vs 80%), a higher rate of neuron loss in CA2 sector (24.3% vs <20%) and in contrast, a higher percentage of CA4 sector neurons than controls (7.9% higher than controls). In HS type 3 category, a slightly higher rate of neuron loss was detected in sector CA1 (26.3% vs the recommended <20%) and CA2 (30% vs 30.2% vs the recommended <25%); sector CA4 registered a lower rate of neuron loss in our cases than recommended (35.7% vs 50%). It is logical to claim that a higher than control neuron count on CA4 might stem from possible miscount of Neu-N positive dentate gyrus neurons as CA4 neurons; these two are intimately close [13]. Morphological differences of these two types of cells are well delineated elsewhere [13]. Whether other discrepancies are a result of low case numbers in each HS group or true phenotypical variance in the Turkish population remains to be seen, preferably in bigger cohorts.

The present study has obvious limitations. The number of cases in the HS type 2 and 3 categories are low, which render any statistical test relatively indecisive. For example, despite the 61.5% neuron loss in CA1 sector of our HS type 2 cases, there is no statistically significant difference between CA1 sectors of our HS type 2 cases and controls (p=0.114). During the actual reporting process, the experienced neuropathologist reviewed all serial slides of the case, including special stains and considered relevant clinical data; also assessed the dentate gyrus neurons and gliosis in the process. Yet the cell counts used in the present study involves a pathologist with relatively low experience in the field that used a single hippocampus section to pick a single representative photograph per CA sector. Relevant literature emphasizes the importance of increasing the numbers of regions of interest (ROI) assessed and having experienced pathologists determine the ROIs [12]. Dentate gyrus abnormalities were also not specifically addressed.

These results are however promising for the utilization of digital pathology-enhanced morphometry as an ancillary technique in pathology. Even a manual Neu-N count done on photomicrographs taken on x10 or x20 magnification with the aid of a simple image processor can aid a regular pathologist with relatively limited experience in hippocampal pathology diagnose hippocampal sclerosis.

Acknowledgement

We sincerely thank Dr. Serdar Balcı for support on statistical analysis.

Author contribution

Study conception and design: FS and GG; data collection: GG, analysis and interpretation of results: FS and GG; draft manuscript preparation: FS and GG. All authors reviewed the results and approved the final version of the manuscript.

Ethical approval

The study was approved by the Hacettepe University Non-interventional Clinical Research Ethics Board (Protocol no. 2022/09-67/31.05.2021).

Funding

The authors declare that the study received no funding.

Conflict of interest

The authors declare that there is no conflict of interest.

REFERENCES

[1] Blumcke I, Aronica E, Miyata H, et al. International recommendation for a comprehensive neuropathologic workup of epilepsy surgery brain tissue: A consensus Task Force report from the ILAE Commission on Diagnostic Methods. Epilepsia. Mar 2016;57(3):348-58. doi:10.1111/epi.13319

[2] Öz BS, F. Pathologic Evaluation of Epilepsy Surgery. Epilepsi. 2012;18(1):53-59. doi:10.5505/epilepsi.2012.88528

[3] Blumcke I, Spreafico R, Haaker G, et al. Histopathological Findings in Brain Tissue Obtained during Epilepsy Surgery. N Engl J Med. Oct 26 2017;377(17):1648-1656. doi:10.1056/NEJMoa1703784

[4] Blumcke I, Thom M, Aronica E, et al. International consensus classification of hippocampal sclerosis in temporal lobe epilepsy: a Task Force report from the ILAE Commission on Diagnostic Methods. Epilepsia. Jul 2013;54(7):1315-29. doi:10.1111/epi.12220

[5] Thom M. Review: Hippocampal sclerosis in epilepsy: a neuropathology review. Neuropathol Appl Neurobiol. Aug 2014;40(5):520-43. doi:10.1111/nan.12150

[6] Thom M, Liagkouras I, Elliot KJ, et al. Reliability of patterns of hippocampal sclerosis as predictors of postsurgical outcome. Epilepsia. Sep 2010;51(9):1801-8. doi:10.1111/j.1528-1167.2010.02681.x

[7] Gunbey C, Soylemezoglu F, Bilginer B, et al. International consensus classification of hippocampal sclerosis and etiologic diversity in children with temporal lobectomy. Epilepsy Behav. Nov 2020;112:107380. doi:10.1016/j.yebeh.2020.107380

[8] Schneider CA, Rasband WS, Eliceiri KW. NIH Image to ImageJ: 25 years of image analysis. Nat Methods. Jul 2012;9(7):671-5. doi:10.1038/nmeth.2089

[9] The Jamovi Project. Version 1.6. 2021. https://www.jamovi.org

[10] Collan Y. Morphometry in pathology: another look at diagnostic histopathology. Pathol Res Pract. Nov 1984;179(2):189-92. doi:10.1016/S0344-0338(84)80126-0

[11] Hamilton PW, Bankhead P, Wang Y, et al. Digital pathology and image analysis in tissue biomarker research. Methods. Nov 2014;70(1):59-73. doi:10.1016/j.ymeth.2014.06.015

[12] Kubach J, Muhlebner-Fahrngruber A, Soylemezoglu F, et al. Same same but different: A Web-based deep learning application revealed classifying features for the histopathologic distinction of cortical malformations. Epilepsia. Mar 2020;61(3):421-432. doi:10.1111/epi.16447

[13] Duvernoy HM. The human hippocampus : functional anatomy, vascularization, and serial sections with MRI. 3rd ed. Springer; 2005:viii, 232 p.